Synthesis and Evaluation of a Novel Series of 2-Chloro-5-((1-methyl-2-(*S*)-pyrrolidinyl)methoxy)-3-(2-(4-pyridinyl)vinyl)pyridine Analogues as Potential Positron Emission Tomography Imaging Agents for Nicotinic Acetylcholine Receptors

LaVerne L. Brown,[†] Santosh Kulkarni,[‡] Olga A. Pavlova, Andrei O. Koren,[†] Alexey G. Mukhin,[†] Amy H. Newman,[‡] and Andrew G. Horti*,[†]

Neuroimaging Research Branch and Medicinal Chemistry Section, Intramural Research Program, National Institute on Drug Abuse, 5500 Nathan Shock Drive, Baltimore, Maryland 21224

Reportedly, 2-[^{18}F]fluoro-A-85380, **1**, a promising radiotracer for imaging the nicotinic acetylcholine receptor (nAChR) by positron emission tomography (PET) in humans, exhibits slow penetration through the blood–brain barrier (BBB) due to its low lipophilicity. A ligand for nAChRs with greater lipophilicity than that of **1** would be potentially more favorable for PET imaging of nAChR due to its faster penetration through the BBB. Herein, a novel series of compounds has been developed based on the high affinity ligand for nAChRs, 2-chloro-5-((1-methyl-2-(*S*)-pyrrolidinyl)methoxy)-3-(2-(4-pyridinyl)vinyl)pyridine, **3b**. The in vitro binding affinities for the new series were found to be in the range of K_i = 9–331 pM. A molecular modeling study showed differences in the comformational profiles and the electronic properties of these compounds, which provides further insight into the structure–activity relationships at nAChR. Lipophilicities of the compounds **3b**–**6b** have been found to be substantially higher than that of **1**. As a result, compounds **3b**–**6b** might exhibit a faster penetration through the BBB than the less lipophilic **1**. The *N*-methyl derivatives **3b** and **6b** demonstrated very high affinities at nAChRs (K_i = 28 and 23 pM, respectively) and will be targets for development of ^{11}CH$_3$-labeled derivatives as radiotracers for PET imaging of nAChRs.

Introduction

Positron emission tomography (PET) is a three-dimensional (3D) imaging technique for the noninvasive measurement of positron-emitting radioisotopes in vivo. The technique requires tracer compounds of physiological interest that are labeled with positron-emitting isotopes. A wide variety of positron-emitting pharmaceuticals incorporating carbon-11 and fluorine-18 have been developed to image brain receptors.[1]

The $\alpha_4\beta_2$ type nicotinic acetylcholine receptors (nAChRs) are the most prominent subtype of nAChRs in mammalian brain.[2] These receptors have been linked to many central nervous system disorders, including Alzheimer's disease, Parkinson's disease, Tourette's syndrome, schizophrenia and attention deficit hyperactivity disorder.[2] For example, decreased density of nAChRs in the hippocampus of patients with schizophrenia and in the cortex of patients with Alzheimer's and Parkinson's diseases has been reported.[3–5] Also, studies show increased density of nAChR in smoking patients when compared to nonsmoking patients.[4,5]

To date, there have been no reports of high specific uptake PET tracers for the study of nAChRs in human subjects. The ^{11}C-labeled nicotine[6] was not satisfactory for such studies due to its high level of nonspecific binding, rapid metabolism, and rapid clearance from the brain. Soon after the discovery of the high affinity nAChR agonist epibatidine,[7] several of its analogues were radiolabeled with PET isotopes C-11 and F-18.[8–10] However, despite the success of [^{18}F]fluorine-labeled epibatidine ([^{18}F]FPH) in animal studies,[12–14] its use in PET studies with humans is prohibited due to high levels of toxicity.[10,11] In the late 1990s, Abbott Laboratories reported break-through publications on the 3-pyridyl ether series of nAChR ligands.[15] Some of these derivatives were equipotent to epibatidine at $\alpha_4\beta_2$ type nAChRs in the in vitro binding assay, but unlike epibatidine, the compounds of the Abbott series exhibited low functional activity at $\alpha_3\beta_x$ subtype nAChRs.[15] The latter receptors are located in the peripheral nervous system and adrenals, and potentially, they are responsible for adverse side effects of nAChR ligands. We speculated that the high affinity for the $\alpha_4\beta_2$ combined with a low functional activity at the $\alpha_3\beta_x$ subtypes of the 3-pyridyl ether series would be advantageous for the development of high affinity radiotracers with low side effects in vivo. Several radiolabeled analogues of A-85380 have been synthesized.[16–20] 2-[^{18}F]-fluoro-A-85380 (**1**) has been used in animal studies[21,22] to image nAChRs, and it is currently the most promising candidate for PET studies in the human brain. Unlike [^{18}F]FPH, **1** shows no adverse side effects at doses substantially exceeding the tracer dose range. Unfortunately, in PET studies with nonhuman primates, **1** exhibited very slow kinetics in the brain.[22,23] Consequently, **1** was deemed less than ideal for occupancy studies of endogenous and exogenous ligands in humans

* To whom correspondence should be addressed. Tel.: 410-550-2916. Fax: 410-550-2724. E-mail: ahorti@intra.nida.nih.gov.
† Neuroimaging Research Branch.
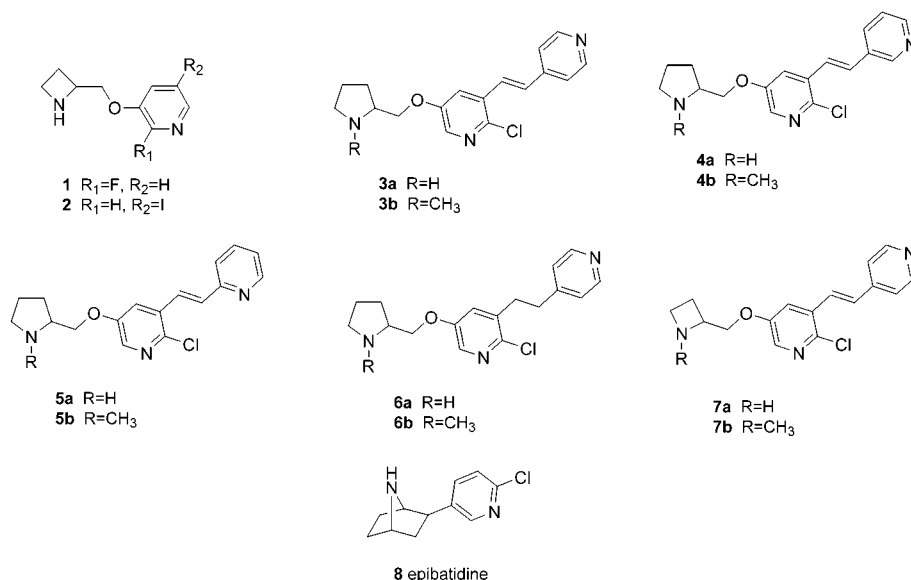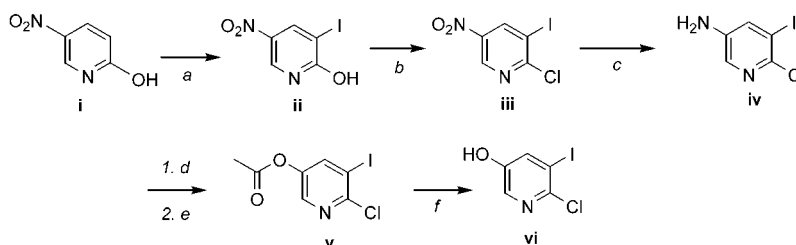‡ Medicinal Chemistry Section.

Figure 1.

Scheme 1[a]

[a] Reagents: (a) I$_2$, K$_2$CO$_3$, DMF; (b) POCl$_3$, quinoline; (c) iron powder, H$_2$O, AcOH; (d) HBF$_4$, NaNO$_2$/H$_2$O; (e) Ac$_2$O; (f) 2 N KOH.

with respect to other nAChR ligands such as nicotine. A radiotracer exhibiting faster penetration through the blood–brain barrier (BBB) should be favored for these PET studies over the currently available radiotracers. Assuming that nAChR ligands penetrate the BBB via a simple diffusion mechanism, we proposed that ligands that are more lipophilic than **1** should cross the BBB at a faster rate. However, radiotracers with higher lipophilicities display increased levels of nonspecific binding and, as a result, produce noisy PET images. For this reason, lipophilic PET radiotracers are not useful unless they exhibit very high binding affinity and correspondingly high specific binding, revealing PET images with lower noise. Therefore, in our investigation of novel PET tracers for nAChRs with more favorable kinetics than that of **1**, we searched for compound(s) with higher lipophilicity and higher binding affinity.

The compound exhibiting the highest affinity for nAChRs in the Abbott series, 2-chloro-5-((1-methyl-2-(*S*)-pyrrolidinyl)methoxy)-3-(2-(4-pyridinyl)vinyl)pyridine, **3b** (K_i = 4.4 pM vs [^{3}H]cytisine[24]), was chosen as a lead molecule in our studies. Because **3b** is significantly more lipophilic than **1** (as estimated by ACD/ Log*D* Suite) and exhibited a higher affinity for nAChRs, we speculated that the radiolabeling of **3b** with ^{11}C would yield a PET radiotracer with faster penetration through the BBB than that of **1**. Here, we report the synthesis of several novel analogues of **3b**. The in vitro binding affinities for compounds **3a,b**−**7a,b** (see Figure 1) have been determined, and the structure-binding

affinity relationships of the series were examined using molecular modeling calculations.
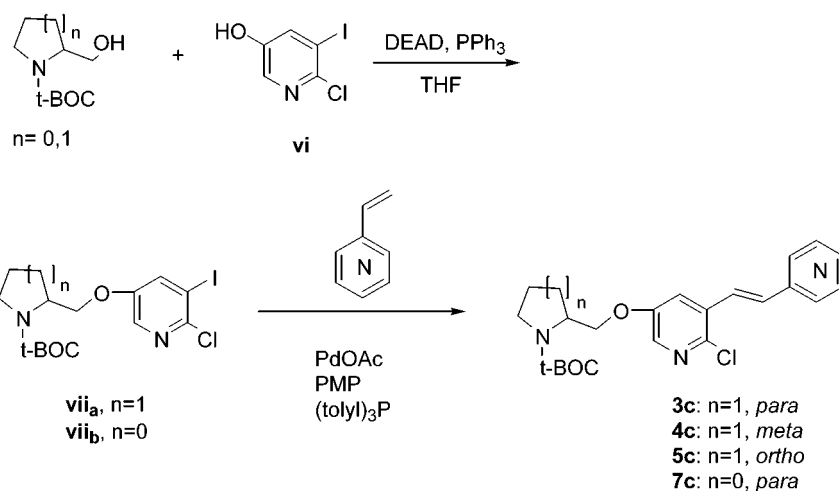
Results and Discussion

Chemistry. The syntheses of **3**−**7** are outlined in Schemes 1−4. In our initial experiments, the intermediate 3-bromo-2-chloro-5-((1-(*tert*-butoxycarbonyl)-2-(*S*)-pyrrolidinyl)methoxy)pyridine[25] gave low yields in the subsequent palladium-assisted Heck coupling with 4-vinylpyridine. Therefore, in anticipation of higher yields and fewer byproducts in the Heck reaction, we synthesized more reactive iodo intermediates (**7a,b**). The iodo intermediates (**7a,b**) were obtained in high yields via Mitsunobu coupling (Scheme 2) of 2-chloro-5-hydroxy-3-iodopyridine (**6**) with 1-(*tert*-butoxycarbonyl)-2(*S*)-azetidinemethanol or 1-(*tert*-butoxycarbonyl)-2(*S*)-pyrrolidinemethanol. A simple five step synthesis of **6** is outlined in Scheme 1.
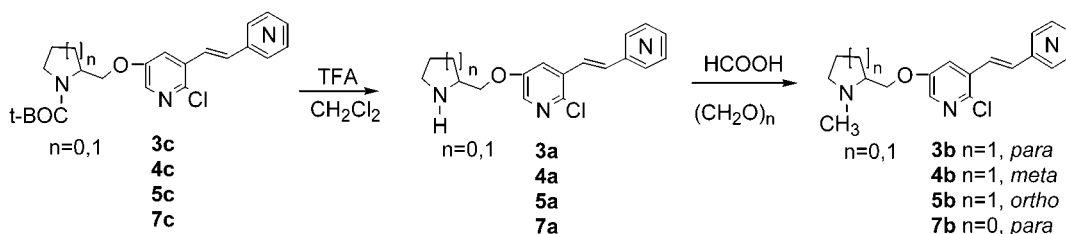
Heck coupling of **7a** with 4-vinylpyridine gave **3c** with 20, 70, and 95% yields in the presence of triethylamine, diisopropylethylamine, or 1,2,2,6,6-pentamethylpiperidine (PMP), respectively (data not shown). Therefore, PMP was used in subsequent syntheses of **4c**, **5c**, and **7c**. Syntheses of **3b**−**7b** were carried out by reductive methylation of **3a,c**−**7a,c** with paraformaldehyde in a solution of formic acid.

Hydrogenation of **3c** in ethyl acetate in the presence of platinum oxide gave **6c**. Noteworthy attempts to obtain **6c** via the hydrogenation of **3c** using Pd/C in methanol or in ethyl acetate were unsuccessful. Instead,
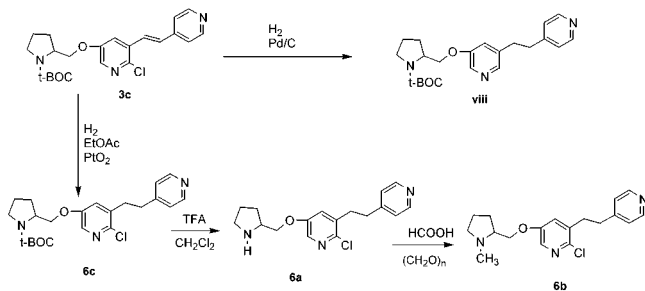
Scheme 2

vi

$n = 0,1$

vii$_a$, n=1
vii$_b$, n=0

3c: n=1, *para*
4c: n=1, *meta*
5c: n=1, *ortho*
7c: n=0, *para*

Scheme 3

n=0,1
3c
4c
5c
7c

n=0,1
3a
4a
5a
7a

n=0,1
3b n=1, *para*
4b n=1, *meta*
5b n=1, *ortho*
7b n=0, *para*

Scheme 4

Table 1. In Vitro Inhibition of 5-[^{125}I]A-85380 Binding to nAChRs in Rat Brain

compd	mean K_i (pM) ± SEM, 23 °C	compd	mean K_i (pM) ± SEM, 23 °C
1	61 ± 5	**5b**	265 ± 5
2	10 ± 1	**6a**	11 ± 1
3a	15 ± 1	**6b**	23 ± 1
3b	28 ± 3	**7a**	9 ± 1
4a	28 ± 1	**7b**	72 ± 6
4b	88 ± 11	**8**	10 ± 1
5a	331 ± 43		

the norchloro derivative (**8**) was obtained in high yields (Scheme 4). The BOC groups of **3c**–**7c** were readily removed by treatment with trifluoroacetic acid (TFA) yielding the TFA salts of **3a**–**7a**.

Lipophilicity. All of the compounds in our series (**3b**–**7b**) are substantially more lipophilic than **1**. Computation of the dissociative partition coefficients in octanol–water system at pH 7.4 (Elog$D_{oct}^{7.4}$) with appropriate software[26] gave for compounds **1**, **3b**, **4b**, **5b**, **6b**, and **7b** the Elog$D_{oct}^{7.4}$ values as follow: −2.09, 1.59, 1.82, 1.55, 1.08, and 1.09. The partition coefficients between octanol and water at pH 7.4 of compounds **1** (log$D_{oct}^{7.4}$ = −2.06) and **3b** (log$D_{oct}^{7.4}$ = 1.60) were also measured by a conventional shake-flask method. The results of the shake-flask method were in remarkably good agreement with calculated results.

Structure–Activity Relationships. It has been reported that compounds **3a** (K_i 39 pM), and, especially, **3b** (K_i 4.4 pM) are extremely high affinity ligands at central nAChRs vs [^{3}H]cytisine at 4 °C.[25] In our studies, competition binding assays were performed using 5-[^{125}I]-iodo-A-85380 (**2**) at 23 °C. Compound **2** has been shown to selectively bind at the $\alpha_4\beta_2$ subtype of nAChRs with high affinity and with high specificity, and it is a

suitable ligand for competition assays at room temperature.[27] All of the compounds in our series, **3b**–**7b**, competitively inhibited **2** in rat P2 membranes at room temperature (23 °C) (Table 1).

Structure–activity relationships, in the *N*-methyl series, **3b**–**5b**, revealed that the para isomer (**3b**) exhibited the highest binding affinity at the $\alpha_4\beta_2$ subtype of nAChRs followed by the meta isomer (**4b**) and then the ortho isomer (**5b**). Reportedly, the phenyl-substituted analogue of **3b** binds with high affinity to nAChRs.[28] These data suggest that the pyridyl nitrogen in the para position may not necessarily enhance affinity. However, the pyridyl nitrogen in the ortho and meta positions may actually decrease optimal binding affinity. Saturation of the olefin bond in the vinylpyridyl moiety of **3a**,**b** resulted in corresponding ethylpyridyl derivatives **6a**,**b** and did not affect affinity for nAChRs. The binding affinities of the N-normethyl derivatives of the pyrrolidine analogues (**3a**–**6a**) were within a 3-fold range of those exhibited by the corresponding N-methyl derivatives (**3b**–**6b**). With the exception of **5a**,**b**, the N-normethyl analogues were more potent than the corresponding N-methylated analogues. The binding affinity exhibited by the azetidinyl analogue, **7a**, was equivalent to that exhibited by epibatidine. Further-

more, **7a** showed the largest difference in binding affinity as compared to its corresponding N-methyl derivative (**7b**). Compound **7a** exhibited an 8-fold higher affinity for $\alpha_4\beta_2$ type nAChRs at 23 °C than **7b**.

Molecular Modeling. The development of a nAChR pharmacophore has been the target of many papers.[24,29–33] These studies have proposed a model for nAChR ligands that contains three essential groups: (i) a cationic center (e.g., a basic or quaternary sp[3] nitrogen atom), (ii) an electronegative atom capable of forming a hydrogen bond (e.g., a pyridine-like nitrogen or a carbonyl oxygen), and (iii) a dummy point or an atom to define a line along which the hydrogen bond may form. Optimal distances between these groups have been proposed. Synthesis of a novel series of high affinity nAChR ligands has necessitated the development of a more-refined pharmacophore. Because the affinity in the present series of compounds appeared to be influenced by structural and electronic effects, these approaches were used to explain the structure–activity relationship.

(−)-Epibatidine (**8**) was used as a template for superimposition studies. Epibatidine possesses a rigid 7-azabicyclo[2.2.1]heptane skeleton and a rotatable bond connecting the chloropyridine ring. A systematic conformational search on epibatidine yielded two low energy conformers. Both conformers showed small conformational energy barriers but differed by a 180° rotation of the chloropyridine ring resulting in an internitrogen distance of 4.4 Å for one conformer and 5.5 Å for the other conformer. Thus, it was difficult to be sure of which low energy conformer of epibatidine was responsible for high affinity binding to nAChRs. A conformational profile analysis of epibatidine (**8**) with molecular mechanics, semiempirical, and ab initio methods indicated that a mixture of all of the conformational minima and some population of the intermediate structures are responsible for the binding of epibatidine to nAChRs.[34] Previous modeling studies have shown that the internitrogen distance for epibatidine was longer than that which was found in nicotine (4.87 Å) and exceeds that of a proposed nAChR pharmacophore.[30] Therefore, the conformer with the internitrogen distance of 5.5 Å was initially selected as a template.

Compounds (**3a,b**–**7a,b**) in this series contain flexible ether linkages connecting two pharmacophoric elements. Thus, it is possible that many conformers of these compounds can be superimposed onto epibatidine. Also, it is well-known that the receptor-bound conformation of the ligands may not be the same as the low energy conformation. Thus, it is important to consider the conformational profiles of the flexible compounds while superimposing onto the template molecule. Generally, it is assumed that for flexible molecules the differences in affinities could be explained based on the superimposibility of the conformers on the template structure. The conformational ensemble within the 2 kcal/mol of the lowest energy conformer for each compound was analyzed by superimposition onto epibatidine, using the sp[3] nitrogen, the nitrogen in the chloropyridine ring, and the centroid of the chloropyridine ring. Each conformer was scored by its root mean square of deviation (RMSD) values. The nAChR pharmacophore elements are approximately in a plane with the chlo-

Table 2. Number of Superimposable Conformers, Distances between Pharmacophore Elements, and RMSD for (−)-Epibatidine and nAChR Ligands

	no. of superimposed conformers		internitrogen distance[b] (Å)	RMSD[c] (Å)
compds	0.0−1.0[a]	1.0−2.0[a]		
8			5.5	
3a	16(40)[d]	20(81)	6.82	0.768
3b	14(36)	22(75)	6.82	0.768
7a	7(20)	20(76)	6.82	0.781
7b	4(15)	23(67)	6.82	0.780
1	11(37)	27(85)	6.66	0.784
2	11(32)	25(90)	6.80	0.781

[a] The energy window in kcal/mol calculated from the lowest energy conformer. [b] Distance between the sp[3] nitrogen and the nitrogen of the chloropyridine ring. [c] RMSD of the three pharmacophore elements from those of (−)-epibatidine. [d] Values in parentheses indicate the total number of conformers in that particular energy window.

ropyridine ring.[35] Therefore, while comparing the conformational profiles of these compounds, the chloropyridine ring was always held coplanar with that of epibatidine. A visual analysis was also included while selecting the conformer for superimposition. This analysis was performed on compounds **3a,b** and **7a,b**. The results from compounds **3a,b** should be applicable to compounds **4a,b**−**6a,b**. Two compounds, **1** and **2**, from our previous studies were used for comparison.[23] The number of conformers of these compounds, which can be superimposed on epibatidine, was partitioned into different energy windows (Table 2). Compounds **3a,b** had nearly identical conformational profiles. However, the conformational profiles of **7a,b** were quite different. Only 26% (4 out of 15) of the conformers of **7b** were superimposable within the 0−1.0 kcal/mol window, but for compound **7a**, 35% (7 out of 20) of the conformers were superimposable. In addition, for compound **7b**, 34% (23 out of 67) of the conformers in the 1.0−2.0 kcal/mol window were superimposed as compared to 26% (20 out of 76) for compound **7a**. Therefore, one explanation for the 8-fold decrease in affinity of **7b** relative to **7a** could be due to the fact that the conformational ensemble contains many higher energy conformers that can be superimposed on epibatidine.

A similar analysis was performed on 2-fluoro-A-85380 and 5-iodo-A-85380 from a previous study.[23] The substitution in the 2-position of the pyridine ring of A-85830 reduced binding affinity to a greater degree than that of a compound substituted at the 5-position. A molecular modeling study on these compounds showed that bulky substitutions on the 2-position affect the geometry of the molecules. As shown in Table 2, a higher number of conformers can be superimposed from the 1.0−2.0 kcal/mol window for **1** than that from 0 to 1.0 kcal/mol window. Thus, for these nicotinic ligands, it appears that the location of binding elements around the nicotinic pharmacophore, as defined by epibatidine, in the conformational ensembles is important for optimal binding affinity.

Once these compounds were superimposed on epibatidine, a difference in the orientation of the N-methyl group of compounds **3b** and **7b** was observed (see Figure 2). The measurement of the angle between the direction of the N-methyl group of compounds **3b** and **7b** shows a difference of approximately 25°. It should be remembered that the N-methyl group in nicotine is essential for activity,[36] whereas N-methylation of epibatidine
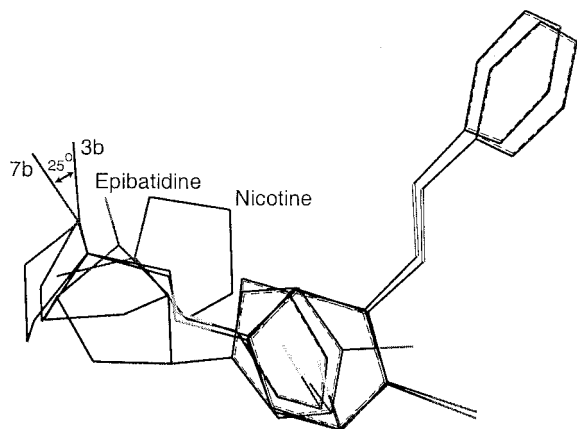
Figure 2. Orientation of the substituent on the sp³ nitrogen of nicotinic compounds. Hydrogens are eliminated from the display for clarity.

reduces activity.[37] This differential effect of the N-methyl group suggests that the nAChR contains a narrow binding pocket that requires proper orientation of the groups for optimal binding affinity. Thus, the N-methyl group in the present series of compounds binds in a different environment, and because of conformational flexibility of the pyridyl ether compounds, the sp³ nitrogen could orient in a different direction.

Furthermore, the internitrogen distance in these conformers was found to be much larger than that which has been proposed for the nicotinic pharmacophore (Table 2).[29] There has been disagreement on this parameter in the literature,[30-32] and the flexibility of these compounds makes the task of identifying a common binding pharmacophore difficult. Therefore, in the absence of a conformationally restricted analogue having a longer internitrogen distance, it is difficult to suggest an optimum internitrogen distance. Overall, the nAChR appears to have wide flexibility with respect to binding of the ligands. The identification of specific types of interactions of the pharmacophore elements with the receptor will help to refine the current understanding of the nAChR pharmacophore.

For example, structure–activity data have shown that the pyridine nitrogen is involved in hydrogen-bonding types of interactions.[38] The sp³ nitrogen was proposed to form an ionic interaction with the anionic site in the receptor.[39] It has also been suggested that the sp³ nitrogen may form cation–π interactions with the aromatic residues in the receptor.[40,41] Recently, Sixma and co-workers reported the X-ray crystal structure of acetylcholine binding protein from a snail, which has high sequence similarity with the N-terminal domain of an α-subunit of nAChRs.[42] This crystal structure may provide clues toward mapping the topology of the ligand binding domain of nAChRs. The binding domain in this protein is lined with hydrophobic residues, and tryptophan-143 was found to be involved in cation–π interactions with the cationic center of the ligand. Also, the cationic binding site was surrounded with aromatic residues, which may interact with the sp³ nitrogen of the ligands. The walls of the binding domain are formed by flat aromatic residues such as tyrosines and tryptophans suggesting that the aromatic ring of the ligands may bind in this region, which is coplanar with the cationic binding site. The molecular modeling data
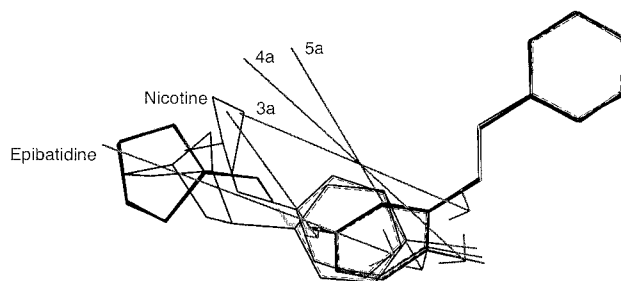
Figure 3. Dipole moments are shown for each compound after superimposition on (−)-epibatidine.

obtained in the present study are consistent with the ligand binding domain of the acetylcholine binding protein.

The compounds **3a**,**b**−**5a**,**b** contain similar ether linkages; however, the substitution at position three of the chloropyridine ring was varied systematically. A preliminary analysis of these compounds showed that the electronic nature of the pendant pyridyl substitution affects binding affinity. The dipole moments of the compounds were visualized and compared with nicotine and epibatidine (Figure 3). A clear trend was observed wherein the more active compound **3a** shows a dipole moment in a similar direction to epibatidine, whereas for compounds **4a** and **5a** the dipole moment was oriented in different directions. Hence, the electron density and its localization also influence nAChR binding affinity. Lack of uniform biological data on a larger scale precluded a quantitative correlation of the electronic descriptors with activity. However, this analysis shows the importance of electrostatic interactions for activity on the nAChR.

Conclusions

Compound **1** is, to date, the most promising candidate for the quantitative imaging of nAChRs in human studies. However, the kinetics exhibited by **1** are likely too slow for occupancy studies of nAChR ligands due to its high hydrophilicity ($\log D_{oct}^{7.4} = -2.1$).

A series of novel analogues of **3a**,**b** were synthesized and evaluated for binding at $\alpha_4\beta_2$ type nAChRs. All of the compounds in our series (**3a**,**b**−**7a**,**b**) exhibited a wide range of affinities for nAChRs ($K_i = 9-331$ pM) measured at room temperature. Compound **7a** was discovered to bind with exceptionally high affinity to $\alpha_4\beta_2$ type nAChRs ($K_i = 9$ pM). The lipophilicities of compounds **3b**−**7b** were within the range of $\log D_{oct}^{7.4} = 1-2$.

Molecular modeling performed with the conformational profile analysis provides further insight into the structure–activity relationship of the present series. The N-methyl group in these compounds influences the activity by altering the conformational mobility and interactions within the receptor pocket. Furthermore, replacement of the vinyl-4-pyridyl substituent of compounds **3a**,**b** with ethyl-4-pyridyl moiety of **6a**,**b** had no substantial effect on binding affinities for nAChRs. However, the position of the nitrogen atom in the vinylpyridyl substituent dramatically affects the binding affinity within the series **3a**,**b**−**5a**,**b**, perhaps due to the changes in the dipole moment orientation.

Because the N-methyl derivatives **3b** and **6b** demonstrated very high affinities at nAChRs ($K_i = 28$ and 23

pM, respectively), they will be targets for development of $^{11}CH_3$-labeled derivatives as radiotracers for PET imaging of nAChRs. High lipophilicity of **3b** and **6b** suggests that their ^{11}C-radiolabeled analogues might exhibit a faster penetration through the BBB than the less lipophilic **1**.

Experimental Section

Chemistry General. All chemicals were purchased from Aldrich, Fluka, or Sigma. Analytical thin-layer chromatographies (TLCs) were run on precoated plates of silica gel (0.25 mm, F254, Alltech). Flash chromatography was conducted using silica gel (230–400 mesh, Merck). Nuclear magnetic resonance (NMR) spectra were recorded on a Bruker (300 MHz) instrument using deuterated solvents and tetramethylsilane (TMS) as an internal standard. Galbraith Laboratories, Inc. performed elemental analyses, and all novel compounds gave satisfactory elemental results (C, H, and N, ±0.4%).

2-Hydroxy-3-iodo-5-nitropyridine (2). 2-Hydroxy-5-nitropyridine, **1**, (14 g, 0.1mol) and potassium carbonate (17 g, 0.1mol) were added to dimethylformamide (DMF; 100 mL, 1.3 mol). Iodine (25.3 g, 0.1mol) was added to the reaction mixture over a 3 min period. After the addition of iodine was complete, the mixture was heated to 80–95 °C for 8 h. The dark reaction mixture was rotary-evaporated to one-half of its initial volume, then cooled to room temperature, and diluted with water (150 mL), and the solid precipitate was filtered. The filtered solution was then made acidic (pH = 5) with glacial acetic acid. The resulting yellow solid was filtered and dried under vacuum to give **2** (11.3 g, 0.043mol, 45% yield). ^1H NMR (acetone-d_6/TMS): δ 8.76 (t, 1H), 8.82 (t, 1H). Anal. calcd for $C_5H_3N_2IO_2$.

2-Chloro-3-iodo-5-nitropyridine (3). 2-Hydroxy-3-iodo-5-nitropyridine, **2**, (70.5 g, 0.27mol) was added to quinoline (16 mL, 0.133mol). The reaction flask was cooled to 5 °C, and phosphoryl chloride (25 mL, 0.27mol) was added dropwise. The mixture was blanketed with argon and heated to 120 °C for 2 h. Upon complete consumption of the precursor, as indicated by TLC, the mixture was cooled to room temperature and 100 mL of H_2O was added. The mixture was then cooled to 0 °C, and the resulting brown solid was filtered. Recrystallization from ethanol gave sand-colored crystals, **3** (60 g, 0.21mol, 78% yield); mp 92–97 °C. ^1H NMR (CDCl$_3$/TMS): δ 8.88 (d, 1H), 9.15 (d, 1H).

5-Amino-2-chloro-3-iodopyridine (4). Compound **3** was added to a solution of H_2O (616 mL) and glacial acetic acid (816 mL). Iron powder (49 g, 0.88mol) was then added to the reaction flask, and the mixture was heated to 65–70 °C. TLC monitoring of the reaction after 5 h indicated no reaction. After 6 h, the exothermic reaction was apparent by a sudden increase in temperature to 85 °C and bubbling in the flask. The bubbling ceased, after approximately 10 min, and the reaction temperature returned to 70 °C. TLC monitoring of the reaction indicated complete consumption of the precursor. H_2O (500 mL) was added to the reaction flask, and the mixture was made basic, pH ≥8, with potassium hydroxide pellets. The mixture was then extracted with ethyl acetate (3 × 250 mL) and evaporated to a yellow solid, **4** (30.55 g, 0.12mol, 68% yield); mp 105–107 °C. ^1H NMR (CDCl$_3$/TMS): δ 3.75 (br s, 2H), 7.51 (d, 1H), 7.85 (d, 1H). Anal. calcd for $C_5H_4N_2ICl$·0.12CH_3CO_2H.

5-Acetoxy-2-chloro-3-iodopyridine (5). Compound **4** (10 g, 39 mmol) was added to HBF$_4$ (59 mL, 50%) and cooled to 0 °C. A solution of sodium nitrite (2.85 g, 41.8 mmol) and H_2O (39 mL) was added dropwise over a period of 1 h. After the addition of sodium nitrite was complete, the mixture was stirred for 1 h at 0 °C. The resulting solid was filtered, washed with diethyl ether (3 × 16 mL), and air-dried for 15 min. The solid was then dissolved in acetic anhydride (47 mL) and heated for 1 h to 70–85 °C. The solvent was evaporated, and the resulting residue was dissolved in diethyl ether (35 mL). The diethyl ether solution was washed with H_2O (4 × 20 mL), dried over MgSO$_4$, and evaporated under reduced pressure.

Compound **5** was obtained as a dark nonviscous liquid (8.32 g, 0.028mol, 72% yield). ^1H NMR (CDCl$_3$/TMS): δ 2.35 (s, 3H), 8.0 (d, 1H), 8.21 (d, 1H).

2-Chloro-5-hydroxy-3-iodopyridine (6). Compound **5** (8.4 g, 2.8 mmol) was added to KOH (50 mL, 2 N) at 5 °C. After it was mixed for 24 h in an ice bath, the unreacted starting material (1.38 g) was removed via filtration. The solution was made acidic, pH 5, with glacial acetic acid, and the resulting solid was filtered. Compound **6** was obtained as a tan powder (4.48 g, 0.018mol, 63% yield); mp 150–160 °C. ^1H NMR (acetone-d_6/TMS): δ 7.81 (d, 1H,), 8.05 (d, 1H).

2-Chloro-3-iodo-5-((1-(*tert*-butoxycarbonyl)-2-(*S*)-pyrrolidinyl)methoxy)pyridine (7a). Diethyl azodicarboxylate (0.72 mL, 4.6 mmol) and triphenylphosphine (1.2 g, 4.6 mmol) were mixed in THF (11.4 mL) at 0 °C, under argon for 30 min. N-BOC-prolinol (0.92 g, 4.6 mmol) and **6** (0.98 g, 3.83 mmol) were then added to the reaction flask, and the mixture was stirred at room temperature for 3 h. The solvent was evaporated under reduced pressure at 55 °C, and the crude oil was purified via flash chromatography (80:20 hexane:ethyl acetate, 300 mL). Compound **7a** was obtained as a yellow oil (1.19 g, 2.7 mmol, 71% yield). ^1H NMR (CDCl$_3$/TMS): δ 1.49 (s, 9H, BOC), 1.87–2.05 (m, 4H), 3.35–3.50 (m, 2H), 4.09–4.22 (m, 3H), 7.7 (d, 1H), 8.1 (d, 1H).

2-Chloro-3-iodo-5-((1-(*tert*-butoxycarbonyl)-2-(*S*)-azetidinyl)methoxy)pyridine (7b). Diethyl azodicarboxylate (0.16 mL, 1.08 mmol) and triphenylphosphine (0.28 g, 1.08 mmol) were mixed in THF (3 mL) at 0 °C, under argon, for 15 min. N-BOC-azetidinylmethanol (0.2 g, 0.88 mmol) and **6** (0.32 g, 0.88 mmol) were then added to the reaction flask in a solution of THF (5 mL). The mixture was stirred at room temperature for 3 h. The solvent was evaporated under reduced pressure at 40 °C, and the crude oil was purified via flash chromatography (50:50 petroleum ether:ethyl acetate, 200 mL). Compound **7b** was obtained as a yellow oil (0.351 g, 0.82 mmol, 94% yield). ^1H NMR (CDCl$_3$/TMS): δ 1.50 (s, 9H, BOC), 2.25–2.4 (m, 2H), 3.8 (m, 2H), 4.15 (m, 1H), 4.35 (m, 1H), 4.55 (m, 1H), 7.7 (d, 1H), 8.1 (d, 1H).

2-Chloro-5-((1-(*tert*-butoxycarbonyl)-2-(*S*)-pyrrolidinyl)methoxy)-3-(2-(4-pyridinyl)vinyl)pyridine (3c) and General Procedure for 3c–5c. Compound **7a** (80 mg, 1.83 mmol) was dissolved in acetonitrile (6.4 mL). The solution was blanketed with argon as vinylpyridine (0.22 mL, 2.08 mmol), PMP (0.36 mL, 2.08 mmol), palladium acetate (0.04 g, 0.18 mmol), and *o*-tritolylphosphine (0.054 g, 0.18 mmol) were added to the reaction flask. The mixture was stirred for 2–24 h at 95 °C until the hihg-performance liquid chromatography (HPLC) monitoring of the reaction indicated complete consumption of the precursor. The solvent was then evaporated at 60 °C. The crude oil was purified via flash chromatography using a short silica gel column (100% diethyl ether, 600 mL).

3c. 95% yield. ^1H NMR (CDCl$_3$/TMS): δ 1.5 (s, 9H), 2.0 (m, 4H), 3.45 (m, 2H), 3.9 (m, 1H), 4.1 (m, 2H), 7.43 (d, 2H), 7.58 (d, 1H), 7.95 (m, 1H), 8.05 (d, 1H), 8.62 (d, 2H).

4c. 52% yield. ^1H NMR (CDCl$_3$/TMS): δ 1.5 (s, 9H), 2.0 (m, 4H), 3.45 (m, 2H), 3.9 (m, 1H), 4.1–4.3 (m, 2H), 7.4–7.6 (m, 3H), 8.0–8.2 (m, 3H), 8.5 (d, 1H), 8.8 (d, 1H).

5c. 95% yield. ^1H NMR (CDCl$_3$/TMS): δ 1.5 (s, 9H), 2.0 (m, 4H), 3.3–3.45 (m, 2H), 3.9 (m, 1H), 4.1 (m, 2H), 7.2 (m, 2H), 7.5 (m, 1H), 7.7 (m, 1H), 7.8 (m, 2H), 8.05 (d, 1H), 8.65 (d, 1H).

2-Chloro-5-((1-(*tert*-butoxycarbonyl)-2-(*S*)-pyrrolidinyl)methoxy)-3-(2-(4-pyridinyl)vinyl)pyridine (7c). Compound **7b** (100 mg, 0.24 mmol) was dissolved in acetonitrile (8 mL). The solution was blanketed with argon as 4-vinylpyridine (0.29 mL, 2.67 mmol), diisopropylethylamine (0.46 mL, 2.64 mmol), palladium acetate (0.05 g, 0.23 mmol), and *o*-tritolylphosphine (0.07 g, 0.23 mmol) were added to the reaction flask. The mixture was stirred for 3 h at 95 °C. TLC monitoring of the reaction indicated complete consumption of the precursor. The solvent was then evaporated via rotary evaporation at 60 °C. The crude oil was purified via flash chromatography on a short silica gel column (100% ethyl acetate, 400 mL) to give a yellow oil (41 mg, 0.102 mmol, 44% yield). ^1H NMR (CDCl$_3$/TMS): δ

1.4 (s, 9H), 2.4 (m, 2H), 3.9 (m, 2H), 4.2 (m, 1H), 4.55 (m, 1H), 4.65 (m, 1H), 7.05 (d, 1H), 7.4 (m, 2H), 7.55 (d, 1H), 7.65 (m, 1H), 8.10 (d, 1H), 8.65 (m, 2H).

2-Chloro-5-(2-(S)-pyrrolidinyl)methoxy)-3-(2-(4-pyridinyl)vinyl)pyridine (3a) and General Procedure for 4a, 5a, and 7a. TFA (2.5 mL, 0.032mol) was added to a solution of **3c** (410 mg, 0.99 mmol) and dichloromethane (10 mL). The reaction was stirred at room temperature overnight. After the reaction was complete, as monitored by TLC, the solvent was evaporated via rotary evaporation at 50 °C. Compound **3a** was obtained as a viscous oil in the form of a TFA salt. Attempts to purify the salt, via flash chromatography on a short silica gel column (600 mL of 90% CH_2Cl_2, 10% CH_3OH, 0.4% NH_4-OH), resulted in significant degradation. Purification via HPLC (82:9:9 0.1% TFA in $H_2O:CH_3CN:CH_3OH$, Preparative PRP-1 Column, 7 mL/min) gave **3a**·TFA (130 mg, 0.41 mmol, 42% yield). For NMR analysis, a portion of **3a**·TFA was dissolved in H_2O (basified with $NaHCO_3$ to pH 8.5) and extracted with diethyl ether to give **3a** in the form of a free base (all other isomers were saved as TFA salts to maintain stability). ^{1}H NMR (acetone-d_6/TMS): δ 2.08−2.2 (m, 4H), 3.55 (m, 2H), 4.25 (m, 1H), 4.6 (m, 2H), 7.47 (d, 1H), 7.6 (d, 2H), 7.65 (d, 1H), 8.0 (d, 1H), 8.15 (d, 1H), 8.62 (d, 2H). Anal. calcd for $C_{17}H_{18}N_3ClO$·2.8TFA·1.5H_2O.

4a·3.5TFA·2H₂O. 58% yield. ^{1}H NMR (acetone-d_6/TMS): δ 1.9−2.9 (m, 5H), 3.5 (m, 1H), 4.1−4.3 (m, 2H), 4.6 (m, 1H), 7.6−7.8 (m, 2H), 8.01−8.16 (m, 3H), 8.8 (m, 2H), 9.13 (d, 1H). Anal. calcd for $C_{17}H_{18}N_3ClO$·3.5TFA·2H_2O.

5a·2.9TFA·1.5H₂O. 47% yield. ^{1}H NMR (acetone-d_6/TMS): δ 2.2−3.0 (m, 5H), 3.56 (m, 2H), 4.3 (m, 1H), 4.56 (m, 2H), 7.7−8.4 (m, 7H), 8.77 (d, 1H).

7a·3.5TFA. 50% yield. ^{1}H NMR (acetone-d_6/TMS): δ 1.4 (s, 9H), 2.4 (m, 2H), 3.9 (m, 2H), 4.2 (m, 1H), 4.55 (m, 1H), 4.65 (m, 1H), 7.05 (d, 1H), 7.4 (m, 2H), 7.55 (d, 1H), 7.65 (m, 1H), 8.10 (d, 1H), 8.65 (m, 2H).

2-Chloro-5-((1-methyl-2-(S)-pyrrolidinyl)methoxy)-3-(2-(4-pyridinyl)vinyl)pyridine (3b) and General Procedure for 4b, 5b, and 7b. Compound **3a** (420 mg, 1.33 mmol) was dissolved in formic acid (2.1 mL). Paraformaldehyde (220 mg) was added, and the reaction mixture was stirred for 5 h at 105 °C. After the reaction was complete, the solvent was evaporated via rotary evaporation at 60 °C. Hydrochloric acid (4.2 mL, 36%) was added to the residue and extracted with diethyl ether (3 × 8 mL). The extract was washed with $NaHCO_3$, dried over $MgSO_4$, and rotary-evaporated at 60 °C to a yellow oil. The oil was rapidly purified by preparative HPLC (PRP-1 column, 84:8:8 0.1% TFA in H_2O:ACN:CH_3OH) forming **3b**·TFA as a viscous oil (81 mg, 0.25 mmol, 19% yield). For NMR analysis, a portion of **3b**·TFA was dissolved in H_2O and extracted with diethyl ether to give **3** in the form of a free base. ^{1}H NMR (CDCl₃/TMS): δ 1.72−1.98 (m, 4H), 2.35−2.45 (m, 1H), 2.51 (s, 3H), 2.71−2.8 (m, 1H), 3.19 (m, 1H), 3.98−4.05 (m, 2H), 6.9 (d, 1H), 7.41 (d, 2H), 7.52 (d, 1H), 7.57 (d, 1H), 8.06 (d, 1H), 8.62 (d, 2H). Anal. calcd for $C_{18}H_{20}N_3ClO$·3TFA·2H_2O·0.3HCl.

4b. Yield 15%. ^{1}H NMR (CDCl₃/TMS): δ 1.72−1.98 (m, 6H), 2.35−2.45 (m, 1H), 2.51 (s, 3H), 2.71−2.8 (m, 1H), 3.19 (m, 1H), 3.98−4.05 (m, 2H), 7.1 (d, 1H), 7.35 (m, 1H), 7.41 (d, 1H), 7.52 (d, 1H), 7.9 (m, 1H), 8.06 (d, 1H), 8.55 (m, 1H), 8.75 (d, 1H). Anal. calcd for $C_{18}H_{20}N_3ClO$·0.7C_3H_6O·0.3H_2O.

5b. Yield 35%. ^{1}H NMR (CDCl₃/TMS): δ 1.72−2.1 (m, 4H), 2.35−2.45 (m, 1H), 2.51 (s, 3H), 2.71−2.8 (m, 1H), 3.19 (m, 1H), 3.98−4.05 (m, 2H), 7.1−7.3 (m, 2H), 7.49 (d, 1H), 7.59 (d, 1H), 7.7 (m, 1H), 7.85 (d, 1H), 8.05 (d, 1H), 8.68 (d, 1H). Anal. calcd. for $C_{18}H_{20}N_3ClO$·0.25TFA·0.8CH_3CN.

7b. Yield 52%. ^{1}H NMR (CDCl₃/TMS): δ 2.1 (s, 6H), 2.5 (s, 3H), 3.0 (m, 1H), 3.5 (m, 3H), 4.1 (m, 2H), 4.4 (m, 1H), 7.05 (d, 1H), 7.3−7.7 (m, 4H), 8.10 (m, 1H), 8.65 (m, 2H). Anal. calcd for $C_{17}H_{18}ClN_3O$·0.7EtOAc·0.3HCOOH.

2-Chloro-5-((1-(tert-butoxycarbonyl)-2-(S)-pyrrolidinyl)methoxy)-3-(2-(4-pyridinyl)ethyl)pyridine (6c). Platinum oxide (195 mg) was added to a solution of ethyl acetate (14 mL) and **3c** (177 mg, 0.4 mmol) and hydrogenated at 50 psi (Parr hydrogenator) for 3 h. Complete consumption of the

precursor was indicated by HPLC. The mixture was filtered through a C18 Sep-Pak, first with ethyl acetate and then with methanol, into two flasks. A norchloro analogue (**8**) was obtained from the methanol fraction (20 mg). Compound **6c** was obtained from the ethyl acetate fraction as a viscous oil (43 mg, 0.1 mmol, 25% yield). ^{1}H NMR (CDCl₃/TMS): δ 1.5 (s, 9H), 1.9−2.09 (m, 4H), 2.98 (m, 4H), 3.39 (m, 2H), 4.05−4.2 (m, 3H), 7.12 (m, 3H), 7.86 (d, 1H), 8.49 (d, 2H).

8. ^{1}H NMR (CDCl₃/TMS): δ 1.5 (s, 9H), 1.9−2.09 (m, 4H), 2.98 (m, 4H), 3.39 (m, 2H), 4.05−4.2 (m, 3H), 7.12 (m, 3H), 7.85 (d, 1H), 7.86 (d, 1H), 8.49 (d, 2H).

2-Chloro-5-(2-(S)-pyrrolidinyl)methoxy)-3-(2-(4-pyridinyl)ethyl)pyridine (6a). TFA (0.9 mL) was added to a solution of **6c** (167 mg, 0.4 mmol) and dichloromethane (10 mL). The mixture was stirred overnight at room temperature. After the reaction was complete, the solvent was rotary-evaporated at 50 °C. Compound **6a**·TFA was obtained as a viscous oil (218 mg). ^{1}H NMR (CDCl₃/TMS): δ 1.25−1.65 (m, 4H), 1.7−2.1 (m, 4H), 3.5 (m, 2H), 3.8−3.95 (m, 3H), 6.98 (d, 1H), 7.12 (d, 2H), 7.95 (d, 1H), 8.56 (d, 2H). Anal. calcd for $C_{17}H_{20}N_3ClO$·2.9TFA·1.5H_2O.

2-Chloro-5-((1-methyl-2-(S)-pyrrolidinyl)methoxy)-3-(2-(4-pyridinyl)ethyl)pyridine (6b). Compound **6a**·TFA (40 mg, 0.126 mmol) was dissolved in formic acid (1 mL). Paraformaldehyde (28 mg) was added, and the reaction mixture was stirred for 5 h at 105 °C. After the reaction was complete, the solution was made basic (pH ≥8) with anhydrous potassium carbonate. The solution was then extracted with ethyl acetate and dried over sodium sulfate. Rotary evaporation at 60 °C gave **6b** as a yellow oil (10 mg, 0.03 mmol, 24% yield). ^{1}H NMR (CDCl₃/TMS): δ 1.7−1.81 (m, 4H), 1.9−2.05 (m, 4H), 2.49 (s, 3H), 2.6−2.7 (m, 2H), 3.85−4.0 (m, 3H), 6.95 (d, 1H), 7.05 (d, 2H), 7.98 (d, 1H), 8.5 (d, 2H). Anal. calcd for $C_{18}H_{22}N_3ClO$·2.5TFA·MeOH·1.3H_2O.

Competition Binding Assay. Competition assays with **2** were performed as described previously.[27] Briefly, the rat brain P2 membrane fractions (5−10 μg of protein) were incubated at 23 °C for 3 h in 0.4 mL of HEPES−salt solution (pH 7.4) in the presence of 10 pM **2** and 9−11 concentrations of test compounds. Nonspecific binding was determined in the presence of (−)-nicotine (300 μM). The binding was terminated by a vacuum filtration through GF/B filters pretreated with 1% polyethyleneimine. Radioactivity was measured using LKB Wallac 1277 γ-counter (efficiency 67%). All assays were carried out in duplicate.

The K_i values were calculated by the Cheng−Prusoff equation based on the measured IC_{50} values and $K_d = 10$ pM for binding of **2**. These K_d values were determined in direct binding assays as described previously.[27] The direct binding assays were performed on the same membrane preparations that were used for the competition assay.

Lipophilicity Estimation. Dissociative partition coefficient ($LogD_{oct}^{7.4}$) determination for **1** and **3b**. Flask-shake method: 0.6 mg of compound **1**[23] or **3b** were added to a vial containing 1 mL of octanol and 1 mL of saline (pH 7.4 was set by addition of 0.1 M sodium phosphate buffer). The vial was shaken for 2.5 h, the mixture was allowed to equilibrate for 48 h at room temperature, and the ligand concentrations in each layer were determined by HPLC analysis. $LogD_{oct}^{7.4}$ values for **1** and **3b** were estimated by dividing the peak area from the octanol layer by the peak area from the saline layer and calculating the log. $LogD_{oct}^{7.4}$ (**1**) = −2.06; $logD_{oct}^{7.4}$ (**3b**) = 1.60.

Molecular Modeling. A molecular modeling study was performed with Sybyl 6.7 running on a Silicon Graphics Octane computer.[43] The structures were built from the standard fragment library in Sybyl. The structures were minimized in a vacuum using a conjugate gradient algorithm until a convergence gradient of 0.001 kcal/mol/Å was reached. The rule-based Gasteiger Marsilli charges were assigned to these molecules during minimization.

The conformational analysis was performed using the systematic search routine. All rotatable single bonds were rotated by 15° increments from 0 to 360°. Conformers having

bad steric interactions were rejected automatically using the van der Waals radii scaling factors of 0.95, 0.87, and 0.65 for general, 1–4, and H-bond interactions. The conformational profile of each compound was evaluated. (−)-Epibatidine (**8**) was used as a template for superimposition, and a conformational search on it was performed analogously. Superimposition was performed by three point alignment using the sp³ nitrogen, the chloropyridine nitrogen, and the centroid of the chloropyridine ring. The best conformer for each compound was selected based on its RMSD value, distance parameters, and visual analysis. It was observed that for all compounds, the lowest energy conformer could not provide a better superimposition on (−)-epibatidine (**8**); hence, conformers with higher than the lowest energy were used for superimposition. The selected conformers were minimized to local minima. The dipole moments were computed after assigning the MOPAC charges calculated from AM1 Hamiltonian.

References

(1) Burns, H. D.; Hamill, T. J.; Eng, W. S.; Hargreaves, R. PET ligands for assessing receptor occupancy *in vivo*. In *Annual Reports in Medicinal Chemistry*; Doherty, A. M., Ed.; Academic Press: San Diego, 2001; Vol. 36, pp 267–276.

(2) Holladay, M. W.; Dart, M. J.; Lynch, J. K. Neuronal Nicotinic Acetylcholine Receptors as Targets for Drug Discovery. *J. Med. Chem.* **1997**, *40*, 4169–4194.

(3) Durany, N.; Zochling, R.; Boissl, K. W.; Paulus, W.; Ransmayr, G.; Tatschner, T.; Danielczyk, W.; Jellinger, K.; Deckert, J.; Riederer, P. Human Post-Mortem Striatal α4β2 Nicotinic Acetylcholine Receptor Density in Schizophrenia and Parkinson's Syndrome. *Neurosci. Lett.* **2000**, *287*, 109–112.

(4) Paterson, D.; Nordberg, A. Neuronal Nicotinic Receptors in the Human Brain. *Prog. Neurobiol.* **2000**, *61*, 75–111.

(5) Newhouse, P. A.; Kelton, M. Nicotinic Systems in Central Nervous Systems Disease: Degenerative Disorders and Beyond. *Pharm. Acta Helv.* **2000**, *74*, 91–101.

(6) Maziere, M.; Comar, D.; Marazano, C.; Berger, G. Nicotine-11C: Synthesis and Distribution Kinetics in Animals. *Eur. J. Nucl. Med.* **1976**, *1*, 255–258.

(7) Spande, T. F.; Garraffo, H. M.; Edwards, M. W.; Yeh, J. C.; Pannell, L.; Daly, J. W. Epbatidine: a novel (chloropyridyl)-azabicycloheptane with potent analgesic activity from an Ecuadorian Poison frog. *J. Am. Chem. Soc.* **1992**, *114*, 3475–3478.

(8) Patt, J. T.; Spang, J. E.; Westera, G.; Buck, A.; Schubiger, P. A. Synthesis and in vivo studies of [C-11]*N*-methylepibatidine: comparison of the stereoisomers. *Nucl. Med. Biol.* **1999**, *26*, 165–173.

(9) Horti, A.; Ravert, H. T.; London, E. D.; Dannals, R. F. Synthesis of a Radiotracer for Studying Nicotinic Acetylcholine Receptors: (±)-Exo-2-(2-[18F]fluoro-5-pyridyl-7-azabio-cyclo[2.2.1]-heptane. *J. Labelled Compd. Radiopharm.* **1996**, *38*, 355–366.

(10) Horti, A. G.; Scheffel, U.; Kimes, A. S.; Musachio, J. L.; Ravert, H. T.; Mathews, W. B.; Zhan, Y.; Finley, P. A.; London, E. D.; Dannals, R. F. Synthesis and Evaluation of N-[11C]Methylated Analogues of Epibatidine as Tracers for Positron Emission Tomographic Studies of Nicotinic Acetylcholine Receptors. *J. Med. Chem.* **1998**, *41*, 4199–4206.

(11) Fisher, M.; Huangfu, D.; Shen, T. Y.; Guyenet, P. G. Epibatidine, an alkaloid from the poison frog Epipedobates tricolor, is a powerful ganglionic depolarizing agent. *J. Pharmacol. Exp. Ther.* **1994**, *270*, 702–707.

(12) Villemagne, V. L.; Horti, A.; Scheffel, U.; Ravert, H. T.; Finley, P.; Clough, D. J.; London, E. D.; Wagner, H. N.; Dannals, R. F. Imaging Nicotinic Acetylcholine Receptor with Fluorine −18-FPH, an Epibatidine Analogue. *J. Nucl. Med.* **1997**, *38*, 1737–1741.

(13) Horti, A. G.; Scheffel, U.; Stathis, M.; Finley, P.; Ravert, H. T.; London, E. D.; Dannals, R. F. (±)-Exo-2-(2-[18F]fluoro-5-pyridyl)-7-azabicyclo[2.2.1]heptane ([18F]-FPH), A New Radioligand for PET Imaging of Nicotinic Acetylcholine Receptors. *J. Nucl. Med.* **1997**, *38*, 1260–1265.

(14) Ding, Y.; Gatley, J.; Fowler, J. S.; Volkow, N. D.; Aggarwal, D.; Logan, J.; Dewey, S. L.; Liang, F.; Carroll, F. I.; Kuhar, M. Mapping of nicotinic acetylcholine receptors with PET. *Synapse* **1996**, *24*, 403–407.

(15) Abreo, M. A.; Lin, N. H.; Garvey, D. S.; Gunn, D. E.; Hettinger, A. M.; Wasicak, J. T.; Pavlik, P. A.; Martin, Y. C.; Donnelly-Robert, D. L.; Anderson, D. J.; Sullivan, J. P.; Williams, M.; Arneric, S. P.; Holladay, M. W. Novel 3-Pyridyl Ethers with subnanomolar affinity for central neuronal nicotinic acetylcholine receptors. *J. Med. Chem.* **1996**, *39*, 817–825.

(16) Kassiou, M.; Ravert, H. T.; Mathews, W. B.; Musachio, J. L.; London, E. D.; Dannals, R. F. Synthesis of 3-[(1-[11C]methyl-2(*S*)-pyrrolidinyl)methoxy]pyridine and 3-[(1-[11C]methyl-2(*R*)-pyrrolidinyl)methoxy]pyridine: radioligands for in vivo studies of neuronal acetylcholine receptors. *J. Labelled Compd. Radiopharm.* **1997**, *39*, 425–431.

(17) Horti, A. G.; Koren, A. O.; Ravert, H. T.; Musachio, J. L.; Mathews, W. B.; London, E. D.; Dannals, R. F. Synthesis of a radiotracer for studying nicotinic acethylcholine receptors: 2-[18F]-fluoro-3-(2(*S*)-azetidinylmethoxy)pyridine (2-[18F]A-85380). *J. Labelled Compd. Radiopharm.* **1998**, *41*, 309–318.

(18) Dolle, F.; Valette, H.; Bottlaender, M.; Hinner, F.; Vaufrey, F.; Guenter, I.; Crouzel, C. Synthesis of a radiotracer for studying nicotinic acethylcholine receptors: 2-[18F]fluoro-3-[(2(*S*)-2-azetidinylmethoxy)pyridine, a highly potent radioligands for in vivo imaging central nicotinic acetylcholine receptors. *J. Labelled Compd. Radiopharm.* **1998**, *41*, 451–463.

(19) Horti, A. G.; Chefer, S. I.; Mukhin, A. G.; Koren, A. O.; Gündisch, D.; Links, J. M.; Kurian, V.; Dannals, R. F.; London, E. D. 6-[18F]-fluoro-A-85380, a novel radioligand for in vivo imaging of central nicotinic acetylcholine receptors. *Life Sci.* **2000**, *67*, 463–469.

(20) Sihver, T.; Fasth, K. J.; Horti, A. G.; Koren, A. O.; Bergstrom, M.; Lu, L.; Hagberg, G.; Lundqvist, H.; Dannals, R. F.; London, E. D.; Nordberg, A.; Langstrom, B. Synthesis and characterization of binding of 5-[Br-76]bromo-3-[[2(*S*)-azetidinyl]methoxy]-pyridine, a novel nicotinic acetylcholine receptor ligand, in rat brain. *J. Neurochem.* **1999**, *73*, 1264–1272.

(21) Horti, A. G.; Scheffel, U.; Koren, A. O.; Ravert, H. T.; Mathews, W. B.; Musachio, J. L.; Finley, P. A.; London, E. D.; Dannals, R. F. 2-[18-F]Fluoro-A-85380, an In Vivo Tracer for the Nicotinic Acetylcholine Receptors. *Nucl. Med. Biol.* **1998**, *25*, 599–603.

(22) Chefer, S. I.; Horti, A. G.; Koren, A. O.; Gundisch, D.; Links, J. M.; Kurian, V.; Dannals, R. F.; Mukhin, A. G.; London, E. D. 2[18-F]F-A-85380: A PET Radioligand for α4β2 Nicotinic Acetylcholine Receptors. *NeuroReport* **1999**, *10*, 2715–2721.

(23) Dolle, F.; Dolci, L.; Valette, H.; Hinner, F.; Vaufrey, F.; Guenter, I.; Fuseau, C.; Coulon, C.; Bottlaender, M.; Crouzel, C. Synthesis and nicotinic acetylcholine receptor in vivo binding properties of 2-[18F]fluoro-3-[(2(*S*)-2-azetidinylmethoxy)pyridine, a new positron emission tomography ligand for nicotinic receptors. *J. Med. Chem.* **1999**, *42*, 2251–2259.

(24) Koren, A. O.; Horti, A. G.; Mukhin, A. G.; Gundisch, D.; Kimes, A. S.; Dannals, R. F.; London, E. D. 2-, 5-, and 6-Halo-3-(2(*S*)-azetidinylmethoxy)pyridines: Synthesis, Affinity for Nicotinic Acetylcholine Receptors, and Molecular Modeling. *J. Med. Chem.* **1998**, *41*, 3690–3698.

(25) Lin, N.-H.; Ho, Y.; Holladay, M. W.; Ryther, K.; Li, Y. 3-Pyridyl-oxymethyl Heterocyclic Ether Compounds Useful In Controlling Chemical Synaptic Transmission. United States Patent 5629325, 1997.

(26) ACD/Log*D* Suite, Advanced Chemistry Development Inc., Toronto, Canada.

(27) Mukhin, A. G.; Gundisch, D.; Horti, A. G.; Koren, A. O.; Tamagnan, G.; Kimes, A. S.; Chambers, J.; Vaupel, D. B.; King, S. L.; Picciotto, M. R.; Innis, R. B.; London, E. D. 5-Iodo-A-85380, an α4β2 subtype-selective Ligand for Nicotinic Acetylcholine Receptors. *Mol. Pharmacol.* **2000**, *57*, 642.

(28) Lin, N.-H.; Abreo, M. A.; Gunn, D. E.; Lebold, S. A.; Lee, E. L.; Wasicak, J. T.; Hettinger, A. M.; Daanen, J. F.; Garvey, D. S.; Campbell, J. E.; Sullivan, J. P.; Williams, M.; Arneric, S. P. Structure–Activity Studies on a Novel Series of Cholinergic Channel Activators Based on a Heteroaryl Ether Framework. *Bioorg. Med. Chem. Lett.* **1999**, *9*, 2747–2752.

(29) Beers, W. H.; Riech, E. Structure and Activity of Acetylcholine. *Nature* **1970**, *228*, 917–922.

(30) Sheridan, R. P.; Nilakantan, R.; Dixon, J. S.; Venkataraghavan, R. The Ensemble Approach to Distance Geometry: Application to the Nicotinic Pharmacophore. *J. Med. Chem.* **1986**, *29*, 899–906.

(31) Glennon, R. A.; Herdon, J. L.; Dukat, M. Epibatidine-Aided Studies Toward Definition of a Nicotinic Receptor Pharmacophore. *Med. Chem. Res.* **1994**, *4*, 461–473.

(32) Glennon, R. A.; Dukat, M. Central Nicotinic Receptor Ligands and Pharmacophores. *Pharm. Acta Helv.* **2000**, *74*, 103–114.

(33) Tonder, J. E.; Hansen, J. B.; Begtrup, M.; Pettersson, I.; Rimvall, K.; Christensen, B.; Ehrbar, U.; Olesen, P. H. Improving the Nicotinic Pharmacophore with a Series of (Isoxazole)methylene-1-azacyclic Compounds: Synthesis, Structure–Activity Relationship, and Molecular Modeling. *J. Med. Chem.* **1999**, *42*, 4970–4980.

(34) Tonder, J. E.; Olesen, P. H.; Hansen, J. B.; Begtrup, M.; Pettersson, I. An Improved Nicotinic Pharmacophore and Stereoselective CoMFA-Model for Nicotinic Agonists Acting at the Central Nicotinic Acetylcholine Receptors Labeled by [³H]-*N*-Methylcabamylcholine. *J. Comput.-Aided Mol. Des.* **2001**, *15*, 247−258.

(35) Campillo, N.; Antonio Paez, J.; Alkorta, I.; Goya, P. A Theoretical Study of Epibatidine. *J. Chem. Soc., Perkin Trans. 2* **1998**, 2665−2669.

(36) Wonnacott, S. Brain Nicotine Binding Sites. *Hum. Toxicol.* **1987**, *6*, 343−353.

(37) Badio, B.; Shi, D.; Garraffo, M.; Daly, J. W. Antinociceptive Effects of the Alkaloid Epibatidine: Further Studies on Involvement of Nicotinic Receptors. *Drug Dev. Res.* **1995**, *36*, 46−59.

(38) Spang, J. E.; Bertrand, S.; Westera, G.; Patt, J. T.; Schubiger, P. A.; Bertrand, D. Chemical Modification of Epibatidine Causes a Switch from Agonist to Antagonist and Modifies its Selectivity for Neuronal Nicotinic Acetylcholine Receptors. *Chem. Biol.* **2000**, *7*, 545−554.

(39) Czajkowski, C.; Karlin, A. Structure of the Nicotinic Receptor Acetylcholine-Binding Site. Identification of Acidic Residues in the δ Subunit Within 0.9 nm of the α Subunit-Binding Site Disulfide. *J. Biol. Chem.* **1995**, *270*, 3160−3164.

(40) Zhong, W.; Gallivan, J. P.; Zhang, Y.; Li, L.; Lester, H. A.; Dougherty, D. A. From ab initio Quantum Mechanics to Molecular Neurobiology: A Cation-π Binding Site in the Nicotinic Receptor. *Proc. Natl. Acad. Sci. U.S.A.* **1998**, *95*, 12088−12093.

(41) Schmitt, J. D.; Sharples, C. G. V.; Caldwell, W. S. Molecular Recognition in Nicotinic Acetylcholine Receptors: The Importance of π-Cation Interactions. *J. Med. Chem.* **1999**, *42*, 3066−3074.

(42) Brejc, K.; van Dijk, W. J.; Klaassen, M.; van der Oost, J.; Smit, A. B.; Sixma, T. K. Crystal Structure of an Ach-Binding Protein Reveals the Ligand-Binding Domain of Nicotinic Receptor. *Nature* **2001**, *411*, 269−276.

(43) *Sybyl6.7*, Tripos Associates, S. Hanley Road, St. Louis, MO.